Supplemental Information

(De)lithiation of Spinel Ferrites Fe_3O_4, $MgFe_2O_4$, and $ZnFe_2O_4$:

A Combined Spectroscopic, Diffraction and Theory Study

David C. Bock[1,†], Killian R. Tallman[2,†], Haoyue Guo[2], Calvin D. Quilty[2], Shan Yan[1], Paul F. Smith[2,3], Bingjie Zhang[2], Diana M. Lutz[2,5,6], Alison H. McCarthy[4,7,8], Matthew M. Huie[4], Veronica Burnett[4], Andrea M. Bruck[2], Amy C. Marschilok[1,2,4], Esther S. Takeuchi[1,2,4], Ping Liu[1], and Kenneth J. Takeuchi[2,4]*

Email: kenneth.takeuchi.1@stonybrook.edu

†equivalent contributions by D.C.B and K.R.T.

[1]Energy and Photon Sciences Directorate, Brookhaven National Laboratory, Upton, NY 11973

[2]Department of Chemistry, State University of New York at Stony Brook, Stony Brook, NY 11794-3400

[3]Present Address: Department of Chemistry, Valparaiso University, Valparaiso, IN 46383-6493

[4]Department of Materials Science and Chemical Engineering, State University of New York at Stony Brook, Stony Brook, NY 11794-2275

[5]Department of Chemistry, Elmira College, Elmira, NY 14901

[6]ExCELS Research Experience for Undergraduates, Stony Brook University, Stony Brook, NY 11794-3400

[7]Department of Mechanical Engineering, The College of New Jersey, Ewing, NJ 08628

[8]Research Experience for Undergraduates: Nanotechnology for Health, Energy and the Environment, Stony Brook University, Stony Brook, NY 11794

Table S1. Rietveld refinement of synchrotron XPD data for synthesized samples of Fe_3O_4, $ZnFe_2O_4$, and $MgFe_2O_4$.

	Fe_3O_4	**$ZnFe_2O_4$**	**$MgFe_2O_4$**	
No. phases	1	1	2	
Crystal System	cubic	cubic	Phase 1 - cubic	Phase 2 - cubic
Space Group	Fd-3m	Fd-3m	Fd-3m	Fd-3m
R_{wp} (%)	3.64	6.35	5.24	
Weight Fraction	1	1	0.57	0.43
a = b = c (Å)	8.3754(2)	8.4306(2)	8.3683(4)	8.440(6)
Size (nm)	9.7(1)	13.2(2)	15.2(2)	2.7(1)
Fe (8a) %	100	-	75(4)	
Mg (8a) %	-	-	25(4)	
Zn (8a) %	-	100	-	
Fe (16d) %	100	100	63(2)	
Mg (16d) %	-	-	37(2)	
Zn (16d) %	-	-	-	
O Coord	0.25280(3)	0.2588(1)	0.25171(1)	

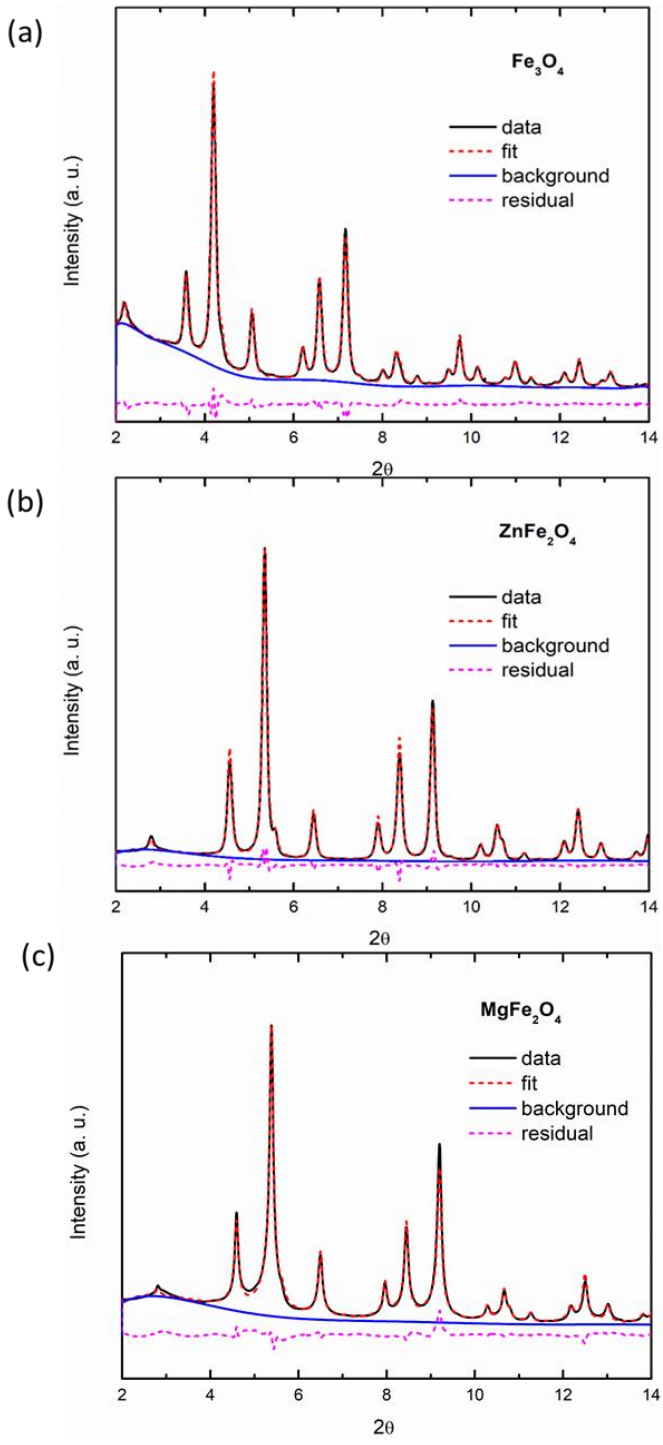

Figure S1. Rietveld refinement of synchrotron XPD data for (a) Fe_3O_4, (b) $ZnFe_2O_4$ and (c) $MgFe_2O_4$.

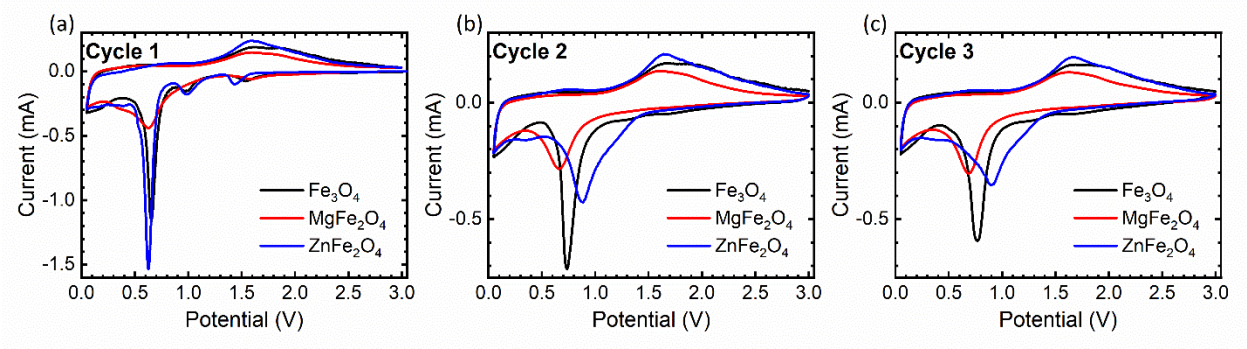

Figure S2. Representative current vs. potential cyclic voltammetry profiles for Fe_3O_4, $MgFe_2O_4$, and $ZnFe_2O_4$. Cycles (a) 1, (b) 2, and (c) 3 are shown using a scan rate of 0.1 mV/s between 0.05 – 3.0 V.

Table S2: Combined R-factor from EXAFS fits of k, k^2 and k^3 k-weights for Fe_3O_4, $MgFe_2O_4$ and $ZnFe_2O_4$.

State	**Fe_3O_4**	**$MgFe_2O_4$**	**$ZnFe_2O_4$ (Fe edge)**	**$ZnFe_2O_4$ (Zn edge)**
unlithiated	0.9	2.1	0.9	2.7
0.5 e- lithiation	1.3	2.0	0.9	2.6
1 e- lithiation	3.9	2.4	0.8	1.1
2 e- lithiation	1.2	2.0	1.1	1.6
4 e- lithiation	0.8	2.1	1.0	1.6
6 e- lithiation	1.9	2.4	1.8	2.5
full lithiation	0.7	2.4	3.2	3.1
4 e- delithiation	3.2	2.7	2.1	0.8
full delithiation	4.2	5.0	3.4	0.9
2^{nd} lithiation	1.2	1.0	0.7	1.9
2^{nd} delithiation	2.9	4.9	2.7	0.8

Table S3: Fitted E_0 from EXAFS fits of k, k^2 and k^3 k-weights for Fe_3O_4, $MgFe_2O_4$ and $ZnFe_2O_4$.

State	**Fe_3O_4**	**$MgFe_2O_4$**	**$ZnFe_2O_4$ (Fe edge)**	**$ZnFe_2O_4$ (Zn edge)**
unlithiated	-1 ± 1	-5 ± 1	-5 ± 1	6 ± 2
0.5 e- lithiation	2 ± 1	-5 ± 1	-1 ± 1	6 ± 1
1 e- lithiation	2 ± 1	-4 ± 1	-3 ± 1	3 ± 3
2 e- lithiation	5 ± 1	-5 ± 1	-1 ± 1	0 ± 1
4 e- lithiation	3 ± 1	-5 ± 2	-2 ± 1	2 ± 1
6 e- lithiation	-3 ± 1	-8 ± 2	-2 ± 2	-2 ± 1
full lithiation	2 ± 1	5 ± 2	4 ± 2	-5 ± 2
4 e- delithiation	-7 ± 7	-2 ± 1	6 ± 2	4 ± 1
full delithiation	-2 ± 1	-2 ± 1	1 ± 1	4 ± 1
2^{nd} lithiation	2 ± 1	5 ± 1	4 ± 1	-4 ± 1
2^{nd} delithiation	-1 ± 2	-3 ± 1	-1 ± 1	4 ± 1

Table S4: Debye-Waller factor fit results for Fe_3O_4, $MgFe_2O_4$ and $ZnFe_2O_4$.

State	Fe_3O_4	$MgFe_2O_4$	$ZnFe_2O_4$ (Fe edge)	$ZnFe_2O_4$ (Zn edge)
unlithiated	(O) 0.010 ± 0.002 (Fe) 0.010 ± 0.002	(O) 0.01 ± 0.01 (Fe) 0.009 ± 0.002 (Mg) 0.009 ± 0.002	(O) 0.005 ± 0.001 (Fe) 0.005 ± 0.001 (Zn) 0.008 ± 0.002	(O) 0.006 ± 0.003 (Fe) 0.006 ± 0.003 (Zn) 0.002 ± 0.004
0.5 e- lithiation	(O) 0.010 ± 0.001 (Fe) 0.010 ± 0.002	(O) 0.01 ± 0.01 (Fe) 0.008 ± 0.002 (Mg) 0.008 ± 0.002	(O) 0.005 ± 0.001 (Fe) 0.005 ± 0.001 (Zn) 0.007 ± 0.002	(O) 0.007 ± 0.003 (Fe) 0.007 ± 0.003 (Zn) 0.002 ± 0.004
1 e- lithiation	(O) 0.010 ± 0.003 (Fe) 0.010 ± 0.002	(O) 0.004 ± 0.004 (Fe) 0.008 ± 0.002 (Mg) 0.008 ± 0.002	(O) 0.006 ± 0.002 (Fe) 0.007 ± 0.001 (Zn) 0.005 ± 0.002	(O) 0.003 ± 0.005 (Fe) 0.007 ± 0.004 (Zn) 0.009 ± 0.005
2 e- lithiation	(O) 0.010 ± 0.001 (Fe) 0.014 ± 0.001	(O) 0.012 ± 0.002 (Fe) 0.012 ± 0.002 (Mg) 0.012 ± 0.002	(O) 0.011 ± 0.002 (Fe) 0.01 ± 0.001 (Zn) 0.01 ± 0.001	(O) 0.012 ± 0.002 (Fe) 0.012 ± 0.002 (Zn) 0.011 ± 0.003
4 e- lithiation	(O) 0.01 ± 0.002 (Fe) 0.01 ± 0.002	(O) 0.01 ± 0.003 (Fe) 0.01 ± 0.003 (Mg) 0.01 ± 0.003	(O) 0.010 ± 0.002 (Fe) 0.011 ± 0.005 (Zn) 0.008 ± 0.006	(O) 0.012 ± 0.002 (Fe) 0.013 ± 0.002 (Zn) 0.010 ± 0.003
6 e- lithiation	(O) 0.004 ± 0.002 (Fe) 0.010 ± 0.002	(O) 0.006 ± 0.003 (Mg) 0.006 ± 0.003 (Fe) 0.007 ± 0.003	(O) 0.010 ± 0.003 (Fe) 0.013 ± 0.004	(O) 0.009 ± 0.002 (Fe) 0.011 ± 0.003 (Zn) 0.011 ± 0.003
full lithiation	(Fe) 0.010 ± 0.001	(Fe) 0.011 ± 0.003	(Fe) 0.010 ± 0.003	(O) 0.011 ± 0.002 (Zn) 0.018 ± 0.002
4 e- delithiation	(O) 0.010 ± 0.09 (Fe) 0.012 ± 0.003	(O) 0.006 ± 0.005 (Fe) 0.006 ± 0.005	(O) 0.002 ± 0.005 (Fe) 0.007 ± 0.002	(O) 0.030 ± 0.004 (Zn) 0.030 ± 0.004
full delithiation	(O) 0.006 ± 0.002 (Fe) 0.006 ± 0.002	(O) 0.007 ± 0.002 (Fe) 0.007 ± 0.002	(O) 0.007 ± 0.002 (Fe) 0.026 ± 0.004	(O) 0.016 ± 0.002 (Zn) 0.016 ± 0.002
2^{nd} lithiation	(Fe) 0.010 ± 0.002	(Fe) 0.010 ± 0.002	(Fe) 0.009 ± 0.002	(O) 0.010 ± 0.001 (Zn) 0.018 ± 0.001
2^{nd} delithiation	(O) 0.008 ± 0.005 (Fe) 0.007 ± 0.005	(O) 0.008 ± 0.005 (Fe) 0.008 ± 0.005	(O) 0.012 ± 0.003 (Fe) 0.023 ± 0.004	(O) 0.004 ± 0.001 (Zn) 0.014 ± 0.009

Table S5: EXAFS fitting results for interatomic distances for Fe_3O_4. Paths associated with the Fe_3O_4, FeO, and Fe metal structures are highlighted in red, blue, and green, respectively. Fe-O paths which are not part of the Fe_3O_4, FeO, or Fe metal structures but were utilized in the model are highlighted in orange.

State	Tetrahedral Iron		Octahedral Iron			
	Fe-O (Å)	Fe-Fe (Å)	Fe-O (Å)	Fe-Fe (Å)	Fe-O (Å)	Fe-Fe Metal (Å)
unlithiated	1.93 ± 0.01 3.61 ± 0.08	3.48 ± 0.02 3.63 ± 0.02	1.98 ± 0.01	3.01 ± 0.01 3.48 ± 0.02		
0.5 e- lithiation	1.92 ± 0.01 3.55 ± 0.05	3.48 ± 0.01 3.63 ± 0.01	2.00 ± 0.01	3.00 ± 0.01 3.48 ± 0.01		
1 e- lithiation	1.94 ± 0.01 3.62 ± 0.01	3.49 ± 0.01 3.64 ± 0.01	2.04 ± 0.01	3.02 ± 0.01 3.47 ± 0.01		
2 e- lithiation			2.08 ± 0.01 3.73 ± 0.04	3.06 ± 0.01		
4 e- lithiation			2.06 ± 0.01 3.62 ± 0.03	3.04 ± 0.01		
6 e- lithiation			2.04 ± 0.01 3.65 ± 0.05	3.09 ± 0.02		2.54 ± 0.02 2.93 ± 0.02
full lithiation						2.45 ± 0.01 2.81 ± 0.01
4 e- delithiation			1.83 ± 0.06	2.79 ± 0.06		2.47 ± 0.04 2.79 ± 0.16
full delithiation			1.93 ± 0.01	3.05 ± 0.03	3.21 ± 0.05	
2nd lithiation						2.46 ± 0.01 2.81 ± 0.01
2nd delithiation			1.94 ± 0.02	3.17 ± 0.06		2.53 ± 0.04

Table S6: EXAFS fitting results for the near neighbors for Fe_3O_4. Paths associated with the Fe_3O_4, FeO, and Fe metal structures are highlighted in red, blue, and green, respectively. Fe-O paths which are not part of the Fe_3O_4, FeO, or Fe metal structures but were utilized in the model are highlighted in orange.

State	Tetrahedral Iron		Octahedral Iron			
	Fe-O	**Fe-Fe**	**Fe-O**	**Fe-Fe**	**Fe-O**	**Fe-Fe Metal**
Unlithiated	1.2 ± 0.2 3.5 ± 0.5	3.5 ± 0.5 1.2 ± 0.2	3.5 ± 0.4	3.5 ± 0.4 3.5 ± 0.4		
0.5 e- Lithiation	1.2 ± 0.1 3.7 ± 0.3	3.7 ± 0.3 1.2 ± 0.1	3.7 ± 0.4	3.7 ± 0.4 3.7 ± 0.4		
1 e- Lithiation	1.2 ± 0.1 3.6 ± 0.3	3.6 ± 0.3 1.2 ± 0.1	3.6 ± 0.4	3.6 ± 0.4 3.6 ± 0.4		
2 e- Lithiation			4.7 ± 0.4 4.7 ± 0.4	9.4 ± 0.7		
4 e- Lithiation			3.8 ± 0.2 3.8 ± 0.2	7.5 ± 0.5		
6 e- Lithiation			1.6 ± 0.2 1.6 ± 0.2	3.4 ± 0.5		1.5 ± 0.4 1.5 ± 0.4
full Lithiation						5.2 ± 0.7 2.1 ± 0.6
4 e- delithiation			1.5 ± 0.8	1.3 ± 0.7		4.6 ± 1.5 0.7 ± 0.3
Full delithiation			2.4 ± 0.2	1.9 ± 0.3	0.4 ± 0.3	
2nd lithiation						5.2 ± 0.9 2.49 ± 0.9
2nd delithiation			2.4 ± 0.5	0.8 ± 0.6		1.1 ± 0.6

Table S7: EXAFS fitting results for the interatomic distances for $MgFe_2O_4$. Paths associated with the $MgFe_2O_4$ structure, a modified structure with all Fe and Mg ions in octahedral sites, and the Fe metal structure, and the FeO structure are highlighted in red, blue, and green, and yellow respectively. Additional Fe-O paths which are not part of these three structures but were utilized in the models are highlighted in orange.

State	Tetrahedral Iron			Octahedral Iron				
	Fe-O (Å)	**Fe-Fe (Å)**	**Fe-Mg (Å)**	**Fe-O (Å)**	**Fe-Fe (Å)**	**Fe-Mg (Å)**	**Fe-O (Å)**	**Fe-Fe Metal (Å)**
unlithiated	1.83 ± 0.01 3.47 ± 0.01	3.46 ± 0.01 3.61 ± 0.01	3.46 ± 0.01	1.97 ± 0.01 3.64 ± 0.01	2.94 ± 0.01 3.46 ± 0.01	2.94 ± 0.01		
0.5 e- lithiation	1.84 ± 0.01 3.47 ± 0.02	3.46 ± 0.02 3.61 ± 0.02	3.46 ± 0.02	1.99 ± 0.01 3.64 ± 0.01	2.94 ± 0.02 3.46 ± 0.02	2.94 ± 0.02		
1 e- lithiation	1.88 ± 0.03 3.47 ± 0.02	3.46 ± 0.02 3.60 ± 0.02	3.46 ± 0.02	2.02 ± 0.03 3.63 ± 0.02	2.94 ± 0.02 3.46 ± 0.02	2.94 ± 0.02		
2 e- lithiation				2.06 ± 0.02 3.67 ± 0.05	3.05 ± 0.01	3.05 ± 0.01		
4 e- lithiation				2.06 ± 0.01 3.68 ± 0.06	3.07 ± 0.02	3.07 ± 0.02		2.54 ± 0.02 2.92 ± 0.02
6 e- lithiation				2.00 ± 0.02 3.60 ± 0.08	3.06 ± 0.02	3.06 ± 0.02		2.52 ± 0.02 2.90 ± 0.02
full lithiation								2.49 ± 0.02 2.79 ± 0.04
4 e- delithiation				1.92 ± 0.01	3.15 ± 0.06			2.53 ± 0.02
full delithiation				2.00 ± 0.01	3.04 ± 0.03		3.10 ± 0.03	
2nd lithiation								2.48 ± 0.01 2.80 ± 0.02
2nd delithiation				1.98 ± 0.01	3.03 ± 0.05		3.12 ± 0.09	

Table S8: EXAFS fitting results for the coordination numbers for $MgFe_2O_4$. Paths associated with the $MgFe_2O_4$ structure, a modified structure with all Fe and Mg ions in octahedral sites, and the Fe metal structure, and the FeO structure are highlighted in red, blue, and green, and yellow respectively. Additional Fe-O paths which are not part of these three structures but were utilized in the models are highlighted in orange.

State	Tetrahedral Iron			Octahedral Iron				
	Fe-O	**Fe-Fe**	**Fe-Mg**	**Fe-O**	**Fe-Fe**	**Fe-Mg**	**Fe-O (Å)**	**Fe-Fe Metal (Å)**
unlithiated	1.1 ± 0.1 3.2 ± 0.4	1.6 ± 0.2 1.1 ± 0.1	1.6 ± 0.2	3.3 ± 0.4 3.3 ± 0.4	1.6 ± 0.2 4.9 ± 0.4	1.6 ± 0.2		
0.5 e- lithiation	1.1 ± 0.1 3.3 ± 0.4	1.6 ± 0.2 1.1 ± 0.1	1.6 ± 0.2	3.3 ± 0.4 3.3 ± 0.4	1.7 ± 0.2 3.3 ± 0.4	1.7 ± 0.2		
1 e- lithiation	1.0 ± 0.3 3.0 ± 0.8	1.5 ± 0.4 0.8 ± 0.2	1.5 ± 0.4	3.0 ± 0.8 3.0 ± 0.8	1.5 ± 0.4 3.0 ± 0.8	1.5 ± 0.6		
2 e- lithiation				4.3 ± 0.5 4.3 ± 0.5	5.7 ± 0.7	2.9 ± 0.4		
4 e- lithiation				2.9 ± 0.5 2.9 ± 0.5	3.8 ± 0.6	1.9 ± 0.3		1.2 ± 0.4 0.9 ± 0.3
6 e- lithiation				1.6 ± 0.4 1.6 ± 0.4	2.1 ± 0.5	1.0 ± 0.2		1.4 ± 0.5 1.1 ± 0.4
full lithiation								4.7 ± 1.3 1.6 ± 1.1
4 e- delithiation				1.7 ± 0.4	0.5 ± 0.4			1.1 ± 0.5
full delithiation				2.1 ± 0.3	0.7 ± 0.3		2.1 ± 0.4	
2nd lithiation								5.0 ± 0.9 1.8 ± 0.9
2nd delithiation				2.4 ± 0.7	1.0 ± 0.9		2.3 ± 0.4	

Table S9: EXAFS fitting results for the interatomic distances for $ZnFe_2O_4$ (Fe edge). Paths associated with the $ZnFe_2O_4$ structure, a modified structure with all Zn and Fe ions in octahedral sites, the FeO structure, and the Fe metal structure are highlighted in red, blue, orange and green, respectively.

State	Octahedral Iron			
	Fe-O (Å)	**Fe-Fe (Å)**	**Fe-Zn (Å)**	**Fe-Fe Metal (Å)**
unlithiated	2.01 ± 0.01 3.55 ± 0.04	3.00 ± 0.01	3.47 ± 0.01	
0.5 e- lithiation	2.01 ± 0.01 3.58 ± 0.04	3.00 ± 0.01	3.48 ± 0.01	
1 e- lithiation	2.02 ± 0.01 3.56 ± 0.01	2.99 ± 0.01	3.45 ± 0.02 2.99 ± 0.01	
2 e- lithiation	2.05 ± 0.01 3.61 ± 0.03	3.03 ± 0.01	3.03 ± 0.01	
4 e- lithiation	2.05 ± 0.01 3.59 ± 0.04	3.02 ± 0.01	3.02 ± 0.01	
6 e- lithiation	1.97 ± 0.02 3.37 ± 0.05	2.97 ± 0.02	2.97 ± 0.02	2.52 ± 0.02 2.90 ± 0.02
full lithiation				2.48 ± 0.02 2.86 ± 0.09
4 e- delithiation	1.87 ± 0.02 3.45 ± 0.02	2.88 ± 0.08		2.48 ± 0.03 2.68 ± 0.08
full delithiation	1.90 ± 0.01 3.49 ± 0.01	3.15 ± 0.03		
2nd lithiation				2.47 ± 0.01 2.80 ± 0.03
2nd delithiation	1.89 ± 0.01 3.48 ± 0.01	3.14 ± 0.03		

Table S10: EXAFS fitting results for the interatomic distances for $ZnFe_2O_4$ (Fe edge). Paths associated with the $ZnFe_2O_4$ structure, a modified structure with all Zn and Fe ions in octahedral sites, the FeO structure, and the Fe metal structure are highlighted in red, blue, orange and green, respectively.

State	Octahedral Iron			
	Fe-O	**Fe-Fe**	**Fe-Zn**	**Fe-Fe Metal (Å)**
unlithiated	5.0 ± 0.4 6.6 ± 0.5	5.0 ± 0.4	5.0 ± 0.4	
0.5 e- lithiation	5.0 ± 0.4 6.6 ± 0.5	5.0 ± 0.4	5.0 ± 0.4	
1 e- lithiation	4.6 ± 0.4 6.1 ± 0.5	4.6 ± 0.4	2.5 ± 0.4 1.2 ± 0.4	
2 e- lithiation	4.9 ± 0.4 6.6 ± 0.5	4.9 ± 0.4	2.5 ± 0.2	
4 e- lithiation	4.6 ± 0.5 6.1 ± 0.6	4.6 ± 0.5	2.3 ± 0.3	
6 e- lithiation	1.9 ± 0.4 2.5 ± 0.6	1.9 ± 0.4	0.9 ± 0.2	2.7 ± 1.2 2.0 ± 0.9
full lithiation				4.3 ± 1.7 3.2 ± 1.3
4 e- delithiation	0.8 ± 0.2 1.1 ± 0.3	1.6 ± 0.5		3.4 ± 0.8 2.5 ± 0.6
full delithiation	2.6 ± 0.3 3.5 ± 0.4	5.2 ± 0.6		
2^{nd} lithiation				4.6 ± 0.7 3.4 ± 0.6
2^{nd} delithiation	3.8 ± 0.4 5.1 ± 0.6	4.8 ± 0.9		

Table S11: EXAFS fitting results for the interatomic distances for $ZnFe_2O_4$ (Zn edge). Paths associated with the $ZnFe_2O_4$ structure, a modified structure with all Fe and Zn ions in octahedral sites, the Zn metal structure, and the ZnO structure are highlighted in red, blue, and green, and yellow respectively. Additional Zn-O paths which are not part of these structures but were utilized in the models are highlighted in orange.

State	Tetrahedral Zn			Octahedral Zn				
	Zn-O (Å)	**Zn-Fe (Å)**	**Zn-Zn (Å)**	**Zn-O (Å)**	**Zn-Fe (Å)**	**Zn-Zn (Å)**	**Zn-O (Å)**	**Zn-Zn Metal (Å)**
unlithiated	2.00 ± 0.02 3.49 ± 0.05	3.50 ± 0.02	3.65 ± 0.03					
0.5 e- lithiation	1.99 ± 0.02 3.49 ± 0.05	3.51 ± 0.02	3.65 ± 0.03					
1 e- lithiation	1.96 ± 0.06 3.49 ± 0.1	3.50 ± 0.09	3.64 ± 0.09	2.07 ± 0.06 3.85 ± 0.01	3.03 ± 0.03	3.03 ± 0.03		
2 e- lithiation				2.05 ± 0.01 3.51 ± 0.04	3.02 ± 0.01	3.02 ± 0.01		
4 e- lithiation				2.06 ± 0.01 3.61 ± 0.06	3.03 ± 0.01	3.03 ± 0.01		
6 e- lithiation				2.04 ± 0.02 3.60 ± 0.05	3.05 ± 0.02	3.05 ± 0.02		
full lithiation							1.92 ± 0.02	2.51 ± 0.02
4 e- delithiation				1.96 ± 0.01 3.76 ± 0.04		3.24 ± 0.05		
full delithiation				1.96 ± 0.01 3.76 ± 0.03		3.21 ± 0.02		
2nd lithiation							1.93 ± 0.01	2.51 ± 0.01
2nd delithiation				1.96 ± 0.01 3.75 ± 0.03		3.21 ± 0.01		

Table S12: EXAFS fitting results for the interatomic distances for $ZnFe_2O_4$ (Zn edge). Paths associated with the $ZnFe_2O_4$ structure, a modified structure with all Fe and Zn ions in octahedral sites, the Zn metal structure, and the ZnO structure are highlighted in red, blue, and green, and yellow respectively. Additional Zn-O paths which are not part of these structures but were utilized in the models are highlighted in orange.

State	Tetrahedral Zn			Octahedral Zn				
	Zn-O	**Zn-Fe**	**Zn-Zn**	**Zn-O**	**Zn-Fe**	**Zn-Zn**	**Zn-O (Å)**	**Zn-Zn Metal (Å)**
unlithiated	2.9 ± 0.5 8.6 ± 1.5	8.6 ± 1.5	2.9 ± 0.5					
0.5 e- lithiation	2.9 ± 0.5 8.6 ± 1.5	8.6 ± 1.5	2.9 ± 0.5					
1 e- lithiation	1.6 ± 0.8 4.7 ± 2.4	4.7 ± 2.4	1.6 ± 0.8	2.0 ± 1.4 2.6 ± 1.9	2.0 ± 1.4	1.0 ± 0.7		
2 e- lithiation				5.0 ± 0.5 6.6 ± 0.7	5.0 ± 0.5	2.5 ± 0.3		
4 e- lithiation				4.9 ± 0.5 6.5 ± 0.7	4.9 ± 0.5	2.4 ± 0.3		
6 e- lithiation				3.4 ± 0.4 4.5 ± 0.5	1.0 ± 0.5	1.7 ± 0.2		
full lithiation							1.1 ± 0.2	4.0 ± 0.2
4 e- delithiation				2.7 ± 0.2 6.1 ± 0.4		4.1 ± 0.2		
full delithiation				2.8 ± 0.2 6.4 ± 0.4		4.2 ± 0.3		
2^{nd} lithiation							1.4 ± 0.2	4.0 ± 0.2
2^{nd} delithiation				2.9 ± 0.2 6.5 ± 0.5		4.3 ± 0.3		

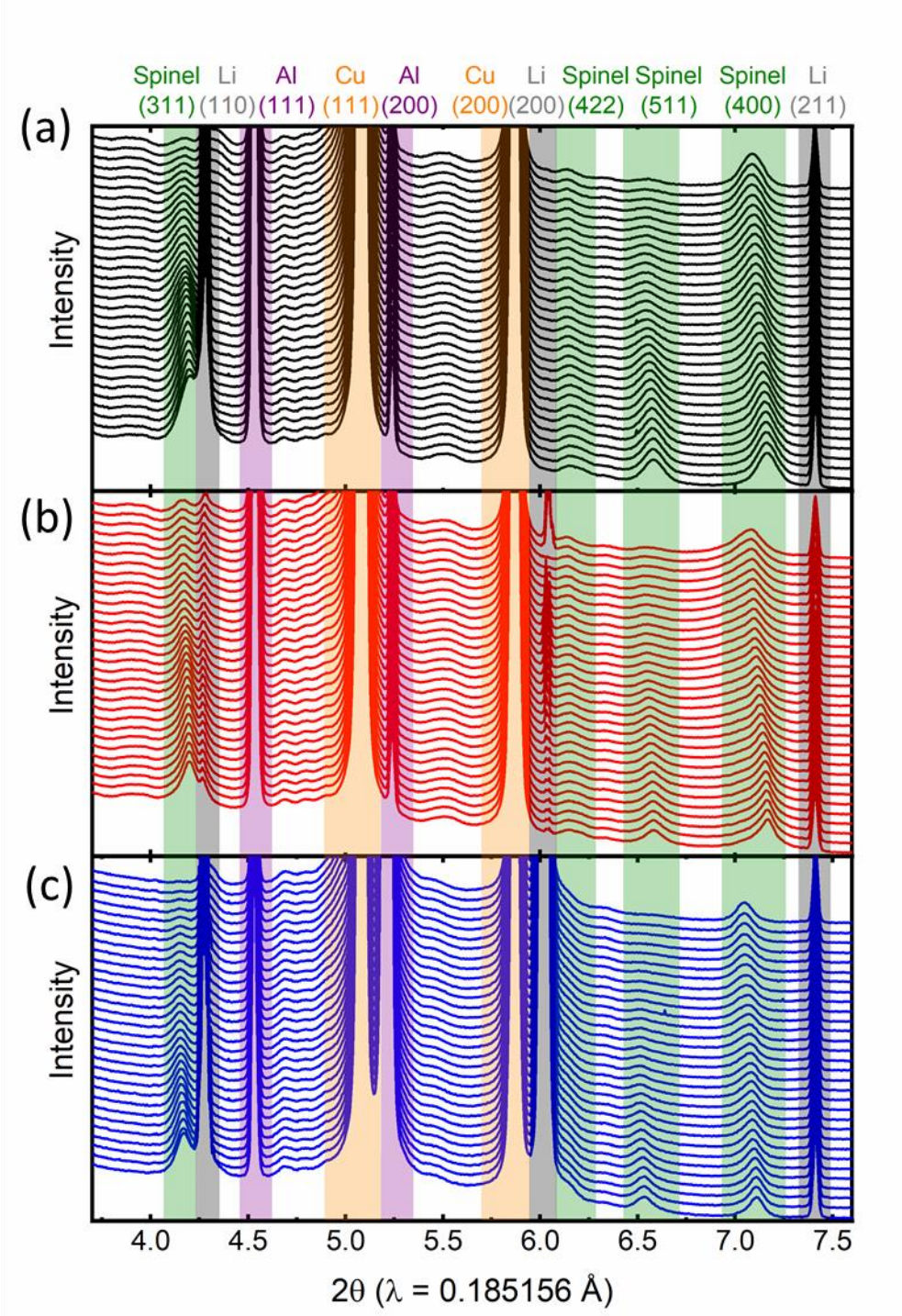

Figure S3. *Operando* synchrotron XRD (a) Fe_3O_4, (b) $MgFe_2O_4$, and (c) $ZnFe_2O_4$. All peaks are indexed to the following phases: spinel, Li metal, Cu metal, and Al metal.

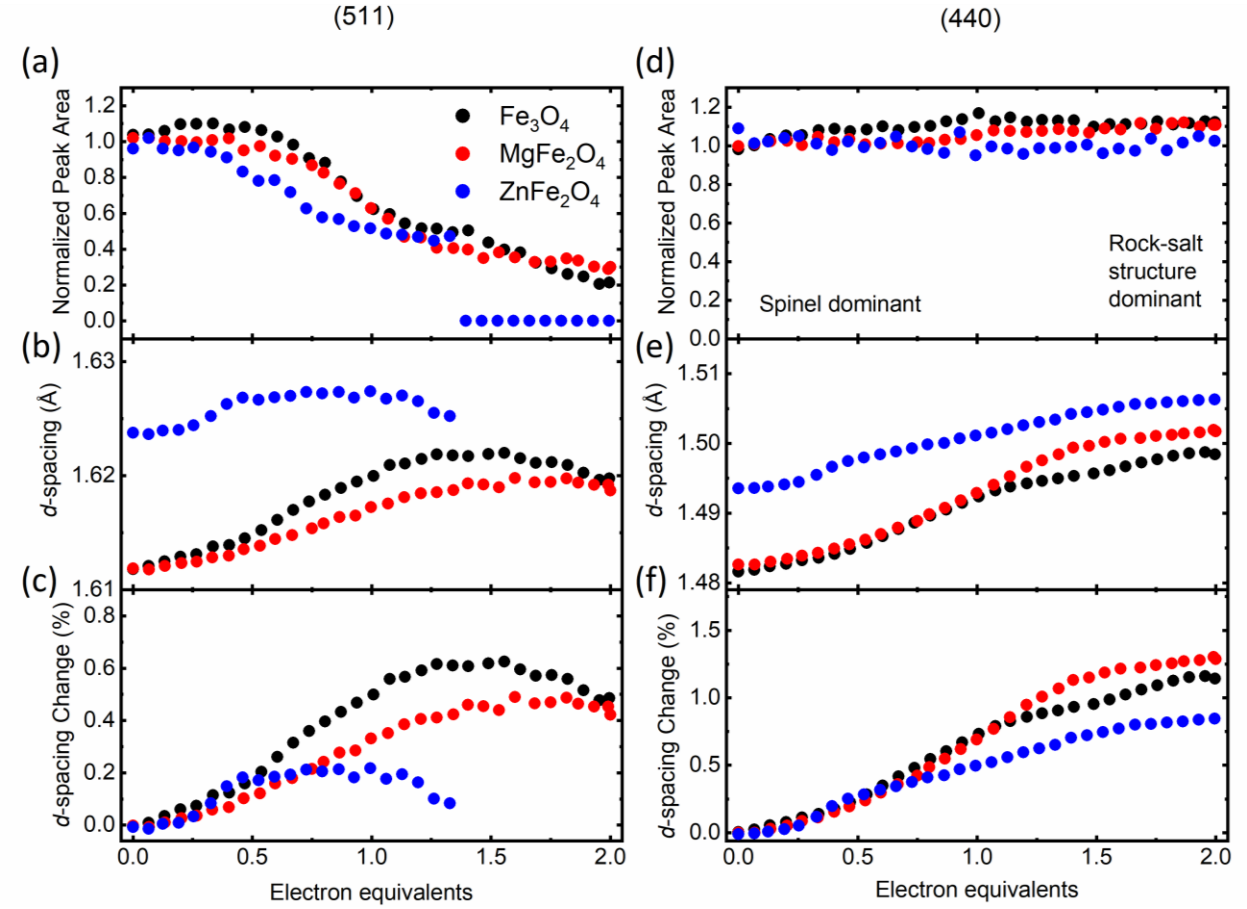

Figure S4. (a, d) Normalized peak areas, (b, e) d-spacing, and (c, f) d-spacing change for (a,b,c) (511) and (d,e,f) (440) reflections from *operando* synchrotron XRD data.

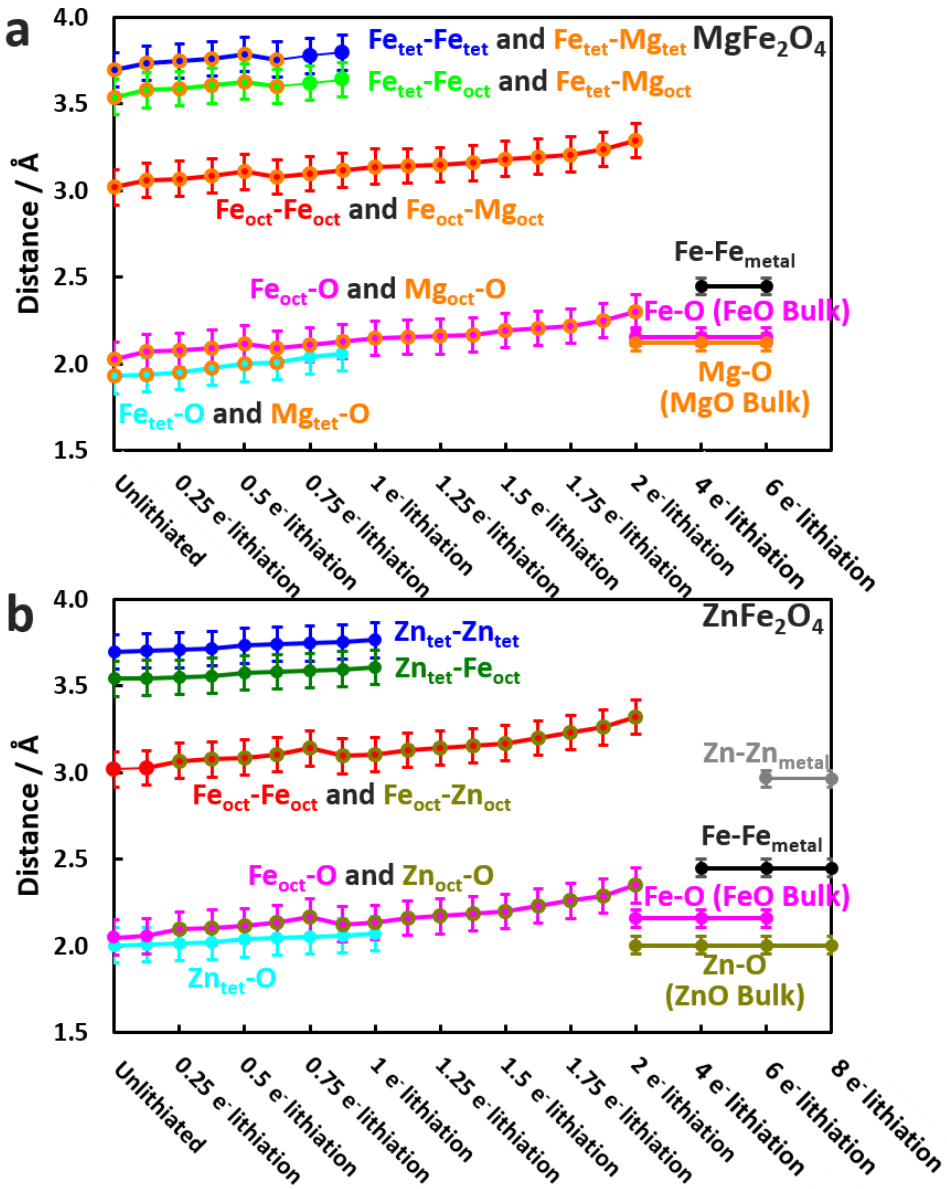

Figure S5. (a) Distances of nearest-neighbors $Fe(Mg)_{tet}$- $Fe(Mg)_{tet}$, $Fe(Mg)_{tet}$- $Fe(Mg)_{oct}$, $Fe(Mg)_{oct}$- $Fe(Mg)_{oct}$, $Fe(Mg)_{oct}$-O, $Fe(Mg)_{tet}$-O in $MgFe_2O_4$ at different lithiation stage and Fe-O in FeO bulk, Mg-O in MgO bulk, Fe-Fe_{metal} in metallic Fe bulk structures to describe the lithiation states after phase separation. (b) Distances of nearest-neighbors Zn_{tet}-Zn_{tet}, Zn_{tet}-Fe_{oct}, $Fe(Zn)_{oct}$- $Fe(Zn)_{oct}$, $Fe(Zn)_{oct}$-O, Zn_{tet}-O in $ZnFe_2O_4$ at different lithiation stage and Fe-O in FeO bulk, Zn-O in ZnO bulk, Fe-Fe_{metal} in metallic Fe bulk, Zn-Zn_{metal} in metallic Zn bulk structures to describe the lithiation states after phase separation.

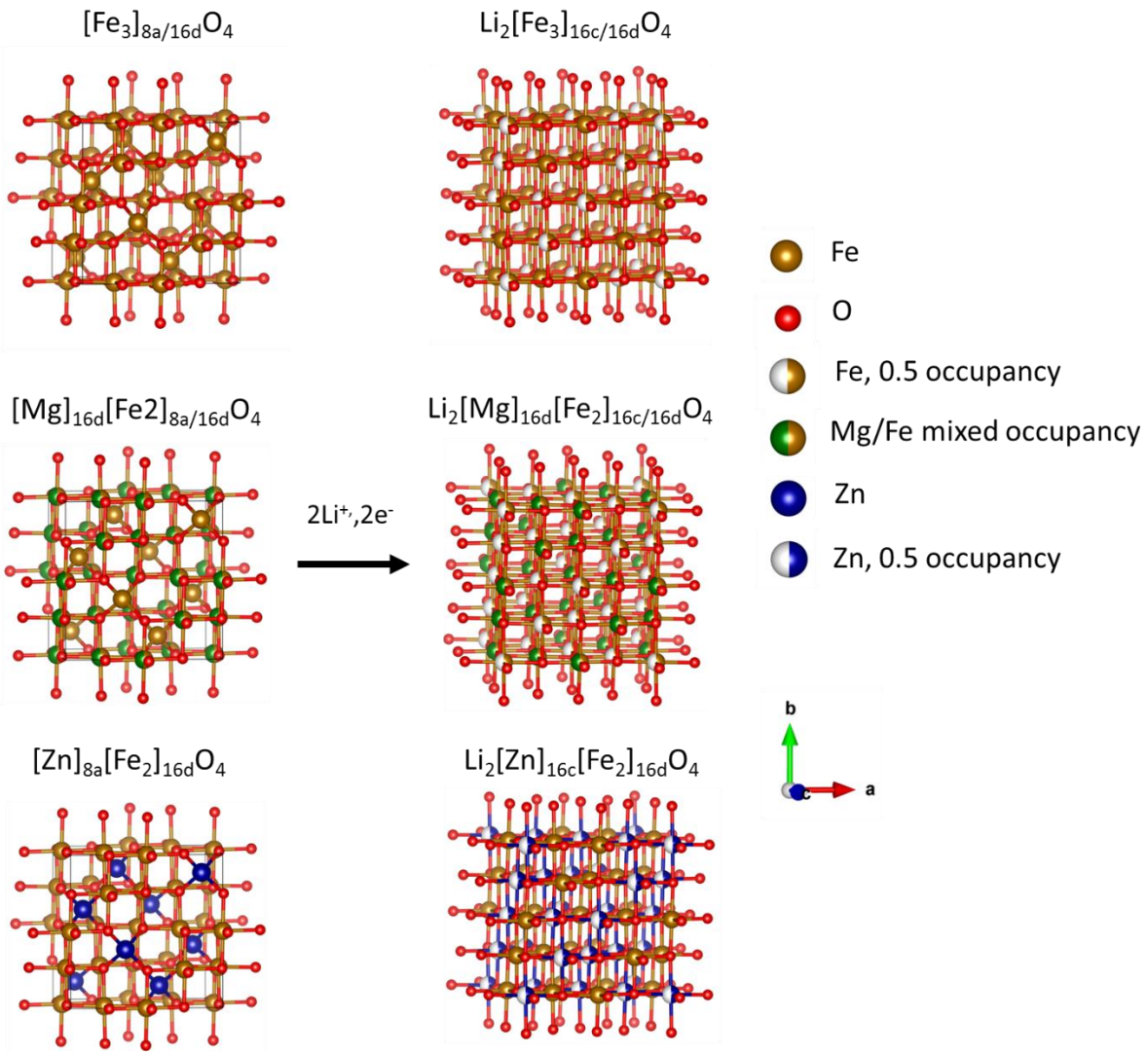

Figure S6. Structures of Fe_3O_4, $MgFe_2O_4$, and $ZnFe_2O_4$ electrode materials in the unlithiated state and after 2 e^- of lithiation.